**Academic Journal of Science and Technology**
ISSN: 2771-3032 | Vol. 20, No. 1, 2026

# MCA-KAN: A Novel Classification Method for Power Quality Disturbances

**Bin Wang**

University of Shanghai for Science and Technology, Shanghai, 200093, China

**Abstract:** With the widespread integration of distributed power systems and renewable energy, power quality disturbance (PQD) problems are becoming increasingly serious. Most existing PQD classification methods rely on the extraction of single time-domain or frequency-domain features, lacking effective cross-domain information fusion, and their classification accuracy significantly decreases under noise interference. To address this issue, this paper proposes a power quality disturbance classification model (MCA-KAN) based on a multi-channel attention mechanism and a KAN network. This model employs parallel time-domain and frequency-domain feature extraction structures, utilizing 1D-CNN and BiLSTM to capture time- and frequency-domain features respectively, and introducing a cross-attention mechanism to achieve adaptive fusion of time-domain and frequency-domain features. Furthermore, the model uses a KANLinear layer for nonlinear mapping to enhance its classification ability and robustness in high-noise environments. To verify the model's robustness, this paper constructs a noisy dataset under three signal-to-noise ratios (SNR=20dB, 30dB, 50dB) and conducts comparative experiments. The results show that the proposed MCA-KAN achieves an accuracy of 97.82% at an SNR of 20dB, and maintains stable recognition performance at higher SNRs. Compared with existing methods, the proposed network outperforms existing methods in terms of classification accuracy and robustness.

**Keywords:** BP Neural Network; Prediction; MCA-KAN; Power Quality Disturbance.

## 1. Introduction

With the increase in power load and the increasing complexity and diversity of electrical equipment, power quality (PQ) has become an important research topic in the operation of power systems [1]. Power quality disturbances (PQD) refer to abnormal fluctuations in voltage, current and frequency in power systems caused by various reasons. There are many types of disturbances, including voltage sags, voltage fluctuations, harmonics, frequency deviations, etc. These disturbances can seriously affect the operational stability of electrical equipment[2], and even lead to equipment damage, production interruption and system failure. Different types of disturbances have different effects on electrical equipment. Accurately identifying and classifying these disturbance types can help power operators take corresponding countermeasures quickly, thereby effectively reducing equipment damage and system failures[3]. Therefore, accurately identifying the types of power quality disturbances under different noise levels is of great significance for the governance of power quality problems and fault diagnosis[4], and has become a research direction of common concern to scholars at home and abroad[5]. The classification methods of power quality disturbances are mainly divided into two categories: traditional signal processing combined with machine learning methods and deep learning methods. (1) In the PQD classification method based on signal processing and machine learning, feature extraction usually adopts Fourier transform (FT)[6], wavelet transform (WT)[7], Stockwell transform (ST)[8], empirical mode decomposition (EMD)[9], Hilbert-Huang transform (HHT)[10] and variational mode decomposition (VMD)[11] and other techniques; the classification stage mainly uses traditional machine learning classifiers, such as artificial neural network (ANN)[12], decision tree (DT)[13] and support vector machine (SVM)[14]. (2) In the PQD method based on deep learning, two main strategies are usually adopted: 1) convert one-dimensional signals into two-dimensional images, and then use mature deep learning models for feature extraction and classification. Common conversion methods include: directly converting the signal into a two-dimensional grayscale image [15], using Wigner-Ville distribution [16] and Gramian Angular Sum Field [17], Trajectory Circle (TC) visualization method [18], and using Markov transition matrix to realize the mapping of signal to image [19]. Although such methods can improve classification accuracy by utilizing the powerful image feature extraction capabilities of deep learning, they may introduce feature information loss during signal reconstruction and require a high level of professional knowledge in the signal conversion process, making the process more complex. 2) Directly inputting the perturbation signal into a one-dimensional convolutional neural network (1DCNN) and a recurrent neural network (RNN) for feature extraction and classification, thereby avoiding the complex signal conversion process. 1DCNN can efficiently extract the spatial features of PQD, while RNN can capture the long and short-term dependency information of the sequence. Reference [20] compared the performance of various typical CNNs and RNNs in classification tasks of 6 classes of single perturbation and 5 classes of compound perturbation, but did not discuss their noise resistance performance. The WT-SFA LSTM, which integrates wavelet multiresolution analysis and attention mechanism, achieves an accuracy close to 100% under high signal-to-noise ratio, but only about 91.8% accuracy under 20dB noise [21]. Although deep learning has made significant progress in power quality disturbance classification tasks, many existing methods mainly rely on time-domain or frequency-domain features, and feature extraction from a single domain may not be able to fully capture the complexity of the disturbance signal. In addition, existing models lack effective mechanisms for handling

cross-domain feature fusion, fail to fully utilize the complementarity of time-domain and frequency-domain information, and the accuracy of power quality disturbance classification will be greatly reduced in high-noise environments. Kolmogorov–Arnold Network (KAN), as a novel network recently proposed, is characterized by using learnable activation functions (such as spline functions) on the edges instead of fixed activation of traditional neurons, thus theoretically approximating complex functions more efficiently. KAN has shown higher accuracy and interpretability than MLP of the same size in small-scale function fitting tasks. In the power field, KAN has been used in fault diagnosis and other directions, and has achieved higher accuracy than CNN, SVM, etc. [22]. To improve the classification performance of power quality disturbances in high-noise environments, this paper proposes a novel power quality disturbance classification model (MCA-KAN). This model extracts time-frequency domain features by fusing temporal and frequency-domain convolutional neural networks and uses a bidirectional long short-term memory (BiLSTM) network to capture the temporal dependencies of signals. Specifically, we introduce a cross-attention mechanism for efficient fusion of time-domain and frequency-domain features, using automatic weighting to enhance the model's focus on important features. KANLinear is introduced into the classification head, utilizing learnable B-spline basis functions to achieve stronger nonlinear mapping capabilities, improving the fitting effect on the boundaries of complex disturbance categories while maintaining controllable parameter quantities. A 25-class PQD synthetic dataset is constructed based on the disturbance definition in IEEE Std 1159-2019, and sufficient experimental validation is conducted under SNR conditions of 20/30/50 dB: the model achieves an accuracy of 97.82% at SNR=20 dB and maintains stable performance at higher SNRs.

## 2. Theoretical Basis and Model Design

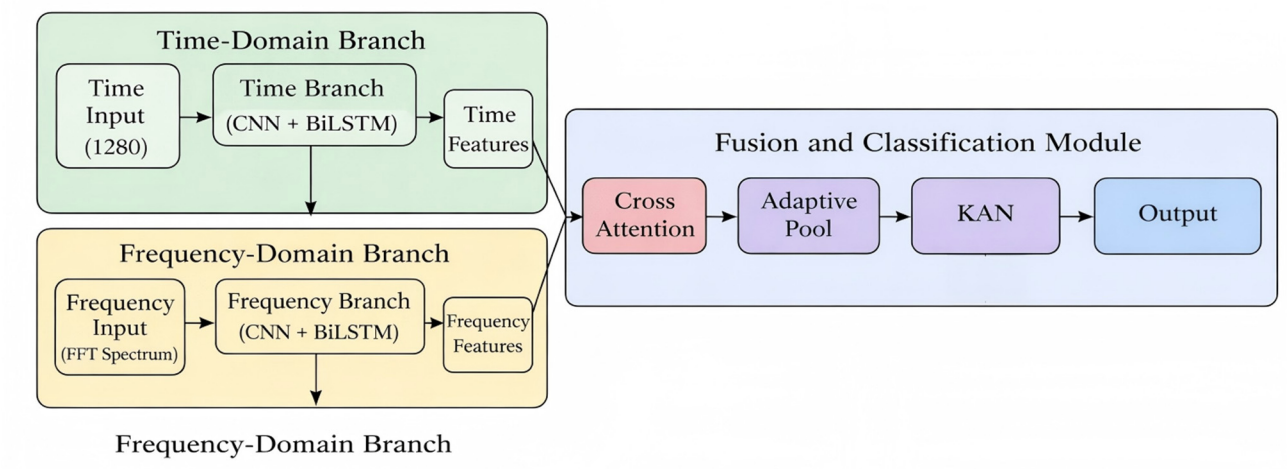


**Fig 1.** Schematic diagram of MCA-KAN model

This model combines the advantages of multi-branch feature extraction and KAN networks, enabling it to capture both local and global features of signals in the time and frequency domains, while also flexibly modeling complex nonlinear mappings. Specifically, the model first performs a Fast Fourier Transform (FFT) on the original power quality disturbance signal, constructing a one-dimensional Convolutional Neural Network (CNN) and a Bidirectional Long Short-Term Memory (BiLSTM) network in the time and frequency domains, respectively. Next, it efficiently fuses these two feature streams using a cross-attention mechanism and obtains a fixed-dimensional vector through adaptive average pooling. Finally, the classification result is output through a KAN module containing linear and B-spline branches.

To eliminate the influence of dimensions and enhance convergence stability, the original sequence is standardized with zero mean and unit variance:

$$\tilde{x}_t = \frac{x_t - \mu_x}{\sigma_x + \epsilon}, \mu_x = \frac{1}{T}\sum_{t=1}^{T} x_t,\ \sigma_x^2 = \frac{1}{T}\sum_{t=1}^{T}(x_t - \mu_x)^2.$$

Subsequently, a Fast Fourier Transform (FFT) is performed on the frequency domain amplitude spectrum $\tilde{x}$. FFT converts the time-domain signal into a frequency-domain amplitude spectrum, thus revealing the signal's frequency components. This method is more computationally efficient than wavelet transform while preserving sufficient frequency information, making it suitable for extracting frequency domain features in power quality disturbance classification. The transformed result is:

$$X_k = \sum_{t=0}^{T-1} \tilde{x}_t\ e^{-j2\pi kt/T}, \hat{x}_k = |X_k|, k = 0, \ldots, T_f - 1.$$

Considering the different saliency of transient and periodic distortions and harmonics/interharmonics in the two domains of PQD, this paper adopts VGG-style one-dimensional convolution stacking in the time and frequency domains respectively, sharing the same hierarchical rhythm (3×Conv+Pool+BN staged stacking), and adopting different channel configurations to match the complexity of the signals in the two domains. The one-dimensional convolution branch structure diagram of time/frequency is shown in Figure 2.

The input to the temporal branch (Time-CNN) is (B, 1, 1280). It uses three convolutional blocks with channels of 32, 64, and 128 respectively; each block contains three Conv1d + ReLU operations with k=3 and p=1, followed by MaxPool1d (stride=2) and BatchNorm1d. After three pooling operations, the length changes from 1280→640→320→160, resulting in a tensor of (B, 128, 160), which is then transposed to obtain a sequence-first format (B, 160, 128). The input to the

frequency branch (Freq-CNN) is (B, 1, 640). It also uses three convolutional blocks, but with channels of 16, 32, and 64, with other settings identical to the temporal branch. The output size is (B, 64, 160), which is transposed to (B, 160, 64).

This "parallel, synchronized, and heterogeneous" design aligns the two branches at the same time step L = 160, facilitating subsequent sequence-level alignment modeling and cross-domain attention interaction.

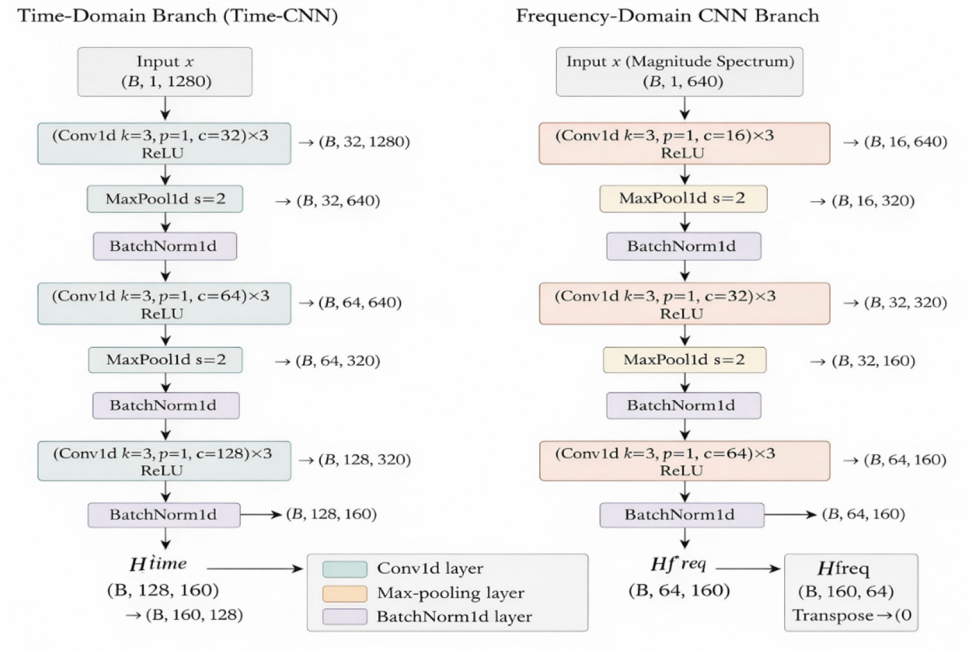


**Fig 2.** Schematic diagram of time/frequency one-dimensional convolution branches

To effectively capture the temporal dependencies of power quality disturbance signals, we employ a Bidirectional Long Short-Term Memory (BiLSTM) network. BiLSTM is used in this model to capture the temporal dependencies of the signal. Unlike traditional unidirectional LSTMs, BiLSTM utilizes both forward and backward temporal information, effectively integrating past and future contextual information. For transient disturbance signals, this bidirectional modeling provides more comprehensive time-series features, thereby improving classification accuracy. Figure 3 shows a schematic diagram of the BiLSTM structure.

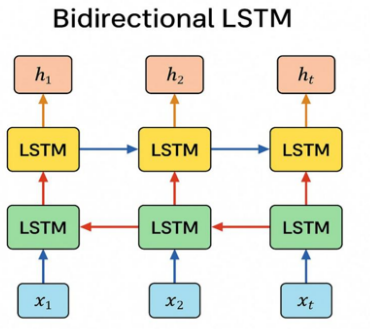


**Fig 3.** Schematic diagram of bidirectional LSTM structure

Given an input sequence {x1, x2, ..., xT}, a standard LSTM is updated using gating and memory units. At time t, it is calculated as follows:

$$i_t = \sigma(W_i x_t + U_i h_{t-1} + b_i)$$
$$f_t = \sigma(W_f x_t + U_f h_{t-1} + b_f)$$
$$o_t = \sigma(W_o x_t + U_o h_{t-1} + b_o)$$
$$\tilde{c}_t = \tanh(W_c x_t + U_c h_{t-1} + b_c)$$
$$c_t = f_t \odot c_{t-1} + i_t \odot \tilde{c}_t$$
$$h_t = o_t \odot \tanh(c_t)$$

Where $i_t$, $f_t$, and $o_t$ are the input gate, forget gate, and output gate, respectively; $c_t$ is the memory cell state, and $h_t$ is the hidden state; $\sigma(\cdot)$ and $\tanh(\cdot)$ are the Sigmoid and hyperbolic tangent functions, respectively, and $\odot$ represents Hadamard element-wise multiplication. The BiLSTM contains two parameter-independent LSTMs: a forward LSTM generates $\overrightarrow{h_t}$, and a backward LSTM generates $\overleftarrow{h_t}$. The representations of these two LSTMs at time t are concatenated to obtain the final context vector.

$$h_t = [\overrightarrow{h_t}; \overleftarrow{h_t}]$$

This simultaneously encodes past and future information, improving the ability to distinguish similar perturbation patterns and enhancing robustness to transient scenarios.

To enable frequency domain cues to actively retrieve the most relevant time-series segments in the time domain, a cross-domain scaled dot product attention mechanism is used, with the frequency domain as the query (Q) and the time domain as the key (K, V). Let

$$\mathbf{Q} = \mathbf{Z}^{\text{freq}}\mathbf{W}_Q, \mathbf{K} = \mathbf{Z}^{\text{time}}\mathbf{W}_K, \mathbf{V} = \mathbf{Z}^{\text{time}}\mathbf{W}_V,$$

Where $\mathbf{W}_Q, \mathbf{W}_K, \mathbf{W}_V \in \mathbb{R}^{128\times d}$ are learnable projections (d = 128 in this paper). Attention is:

$$\text{Attn}(\mathbf{Q}, \mathbf{K}, \mathbf{V}) = \text{softmax}(\frac{\mathbf{Q}\mathbf{K}^\top}{\sqrt{d}})\mathbf{V}.$$

Focus on M-head splicing and channel-dimensional stitching:

$$\mathbf{F} = Concat(head_1, \dots, head_M)\mathbf{W}_O.$$

And linearly mapped back to $2H_2 = 128$ dimensions. This mechanism allows the spectral peaks, energy bandwidth, and amplitude/frequency modulation features in the frequency domain to align and "point" to the most discriminative transient segments or stable segments in the time domain, thereby achieving cross-domain complementarity. To further enhance channel discriminability, channel recalibration (SE form) is added after multi-head splicing: global average pooling in the time dimension is first performed on $\mathbf{F} \in \mathbb{R}^{L\times 128}$ to obtain $\mathbf{s} \in \mathbb{R}^{128}$.

$$\mathbf{s} = \sigma\big(\mathbf{W}_2\,\mathrm{ReLU}(\mathbf{W}_1\,GAP(\mathbf{F}))\big) \in \mathbb{R}^{2H}$$

Here, GAP is channel-dimensional global average pooling, followed by element-level recalibration $\tilde{\mathrm{F}} = \mathrm{F} \odot \mathrm{s}$. Finally, time-dimensional global average pooling (GAP) is performed on $\tilde{\mathrm{F}}$ to obtain

$$\mathbf{z} = GAP_{time}(\tilde{\mathbf{F}}) \in \mathbb{R}^{2H}.$$

Furthermore, a KANLinear (B-spline kernelized linear layer) is used instead of a conventional fully connected layer. The KANLinear layer is one of the key innovations in the MCA-KAN model. Traditional fully connected layers typically use a fixed activation function (such as ReLU), while the KANLinear layer performs nonlinear transformations using B-spline kernelization. This method can more effectively approximate complex functions, especially suitable for nonlinear features in power quality disturbance classification. In addition, the KANLinear layer optimizes feature transformations through residual connections, enhancing the model's interpretability and adaptability. A KAN classification head is constructed from 128 to 64 to 25, enhancing nonlinear discrimination and interpretability while maintaining controllable parameter counts. For each input $[a,b] = [-1,1]$ B-spline basis $\{B_{i,m}(z_i)\}_{m=1}^{M}$ in this paper, $M = \text{grid_size} + \text{spline_order} = 5 + 3 = 8$of degree k is constructed on the grid [a,b]=[-1,1] with a step size h, and is stably computed using Cox-de Boor recursion. The c-th output (category logits) is represented as

$$y_c = \underbrace{\sum_{i=1}^{128} w_{ci}^{\text{base}}\ \phi(z_i)}_{\text{Baseline branch}} + \underbrace{\sum_{i=1}^{128} \backslash big\,(\mathbf{w}_{c,i}^{\text{spline}} \backslash big)^{\top} \mathbf{b}_i(z_i)}_{B\ spline\ branch}$$

Where $\phi(\cdot)$ adopts SiLU, $\mathbf{b}_i(z_i) = [B_{i,1}(z_i), \ldots, B_{i,M}(z_i)]^{\top}$To enhance the scale adaptation of the spline response of each channel, a learnable channel scale coefficient $\alpha_{c,i}$: $\mathbf{w}_{c,i}^{\text{spline}} \leftarrow \alpha_{c,i}\,\mathbf{w}_{c,i}^{\text{spline}}$. KAN followed by Softmax obtains the class probability $\mathbf{p} \in \mathbb{R}^{25}$. Figure 4 is a schematic diagram of the KAN classification head structure.

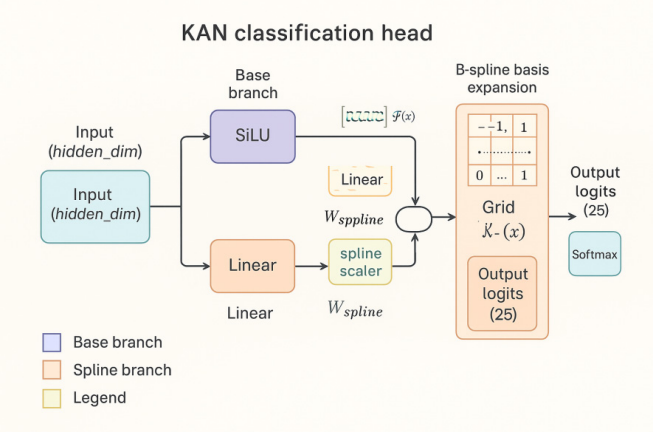


**Fig 4.** Schematic diagram of the KAN classification head structure

# 3. Experiments and Analysis

## 3.1. Dataset Construction

This study constructed the PQD dataset in accordance with IEEE Std1159-2019 standards. All disturbance parameters were randomly generated as specified in the standard. Using Python, disturbance signals were generated with a fundamental frequency of 50 Hz and a sampling rate of 6400 Hz, with a sampling interval of 10 cycles (0.2 s), resulting in a total of 1280 sampling points. A total of 25 different types of PQD signals (C1-C25) were generated, including 10 single disturbances and 15 composite disturbances. Each disturbance category was sampled 1000 times, totaling 25,000 samples. Since real PQDs typically contain noise, Gaussian white noise with signal-to-noise ratios (SNRs) of 20 dB, 30 dB, and 50 dB was added to enhance data authenticity, thereby testing the model's noise resistance and generalization capabilities. The SNR refers to the ratio of signal to noise in an electronic device or system.

**Table 1.** The mathematical models and related parameters for each disturbance category

| Number | Categories | Mathematical model | Parameters |
|---|---|---|---|
| C1 | Normal | $y(t) = [1 \pm \alpha\{u(t-t_1) - u(t-t_2)\}]sin(2\pi ft)$ | $\alpha \le 0.1, T \le t_2 - t_1 \le 9T$ |
| C2 | Swell | $y(t) = [1 + \alpha\{u(t-t_1) - u(t-t_2)\}]sin(2\pi ft)$ | $0.1 \le \alpha \le 0.8, T \le t_2 - t_1 \le 9T$ |
| C3 | Sag | $y(t) = [1 - \alpha\{u(t-t_1) - u(t-t_2)\}]sin(2\pi ft)$ | $0.1 \le \alpha \le 0.9, T \le t_2 - t_1 \le 9T$ |
| C4 | Interruption | $y(t) = [1 - \alpha\{u(t-t_1) - u(t-t_2)\}]sin(2\pi ft)$ | $0.9 \le \alpha \le 1, T \le t_2 - t_1 \le 9T$ |
| C5 | Harmonics | $y(t) = \alpha_1 sin(2\pi ft) + \alpha_3 sin(6\pi ft) + \alpha_5 sin(10\pi ft) + \alpha_7 sin(14\pi ft)$ | $0.05 \le \alpha_3, \alpha_5, \alpha_7 \le 0.15, \sum \alpha_i^2 = 1$ |
| C6 | Flicker | $y(t) = [1 + \alpha_f sin(2\pi\beta t)]sin(2\pi ft)$ | $0.1 \le \alpha^f \le 0.2, 5Hz \le \beta \le 20Hz$ |
| C7 | Pulse | $y(t) = \sin(2\pi ft) + \mathrm{sign}(\sin(2\pi ft)) \cdot ae^{-\frac{(t-t_1)}{\tau}}\{u(t-t_1) - u(t-t_2)\}\sin(2\pi ft)$ | $0.2 \le \alpha \le 1.0, 1ms \le \tau \le 5msT/20 \le t_2 - t_1 \le T/10$ |
| C8 | Oscillation transients | $y(t) = \sin(2\pi ft) + ae^{-\frac{(t-t_1)}{\tau}}\sin(2\pi f_n t)\{u(t-t_1) - u(t-t_2)\}$ | $0.1 \le \alpha \le 0.8, 0.5T \le t_2 - t_1 \le 3T, 8ms \le \tau \le 40ms, 300Hz \le f_n \le 900Hz$ |
| C9 | Periodic notch | $y(t) = \sin(\omega t) - \mathrm{sign}(\sin(2\pi ft)) \cdot \left\{\sum_{n=0}^{9} k\left[u(t-(t_1-0.02n)) - u(t-(t_2-0.02n))\right]\right\}$ | $0.1 \le k \le 0.4, 0 \le t_1, t_2 \le 0.5T, 0.01T \le t_2 - t_1 \le 0.05T$ |
| C10 | Spikes | $y(t) = \sin(\omega t) + \mathrm{sign}(\sin(2\pi ft))^{*} \left\{\sum_{n=0}^{9} k\left[u(t-(t_1-0.02n)) - u(t-(t_2-0.02n))\right]\right\}$ | $0.1 \le k \le 0.4, 0 \le t_1, t_2 \le 0.5T, 0.01T \le t_2 - t_1 \le 0.05T$ |

Under normal conditions, a higher SNR indicates better voltage signal quality, meaning the signal is clearer relative to noise, while a lower SNR suggests poorer signal quality and greater noise interference. After generating the dataset, the

training set, validation set, and test set were divided in a 14:3:3 ratio. Three fixed-noise datasets with SNRs of 20 dB, 30 dB, and 50 dB were generated. The mathematical models and related parameters for each disturbance category are detailed in Table 1.

The simulation platform environment is configured with Windows 10 operating system (13th Gen Intel® Core™ i5-13600KF (3.50 GHz) and NVIDIA GeForce RTX 4070 SUPER-12GB GPU), utilizing the PyTorch deep learning framework. During training, Adam was selected as the optimizer with an initial learning rate of 0.0003, batch size of 128, and 50 iterations, with classification accuracy serving as the evaluation metric.

Throughout the experiment, the hyperparameters used in this model are shown in Table 2.

**Table 2.** Hyperparameter Configuration

| hyperparameter | Set value |
|---|---|
| Convolutional layer channel count | timeconv: 32, 64, 128, spaceconv: 16, 32, 64 |
| Convolution kernel size | 3 |
| LSTM hidden layer size | 128, 64 |
| Learning Rate | 0.0003 |
| batch size (BatchSize) | 128 |

## 3.2. Model Performance Comparison

Figure 5, 6, and 7 present the confusion matrices of the proposed model under varying noise levels. The matrices demonstrate that as the signal-to-noise ratio (SNR) increases, the model's classification accuracy progressively improves, consistently maintaining above 97.00%, indicating strong noise resistance. However, the model's performance shows slight deterioration at lower SNRs. Specifically, the classification accuracy reaches 99.39% at 30dB and 99.56% at 50dB, but drops to 97.82% at 20dB. The matrices reveal that partial noise interference reduces accuracy. This occurs because photonic quantum dots (PQDs) may blur or mask useful signal features at low SNRs, hindering accurate feature extraction. The resulting feature obscuration ultimately leads to lower classification accuracy.

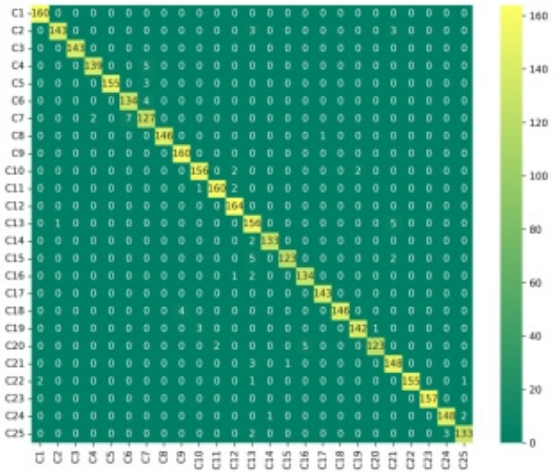

**Fig 5.** 20dB

Table 3 presents the classification accuracy of the MCA-KAN model under varying noise levels, with comparisons to other mainstream models. To validate the proposed model's superiority, we selected several representative models for comparison, including CNN, LSTM, TCN+LSTM, and CNN-Transformer.

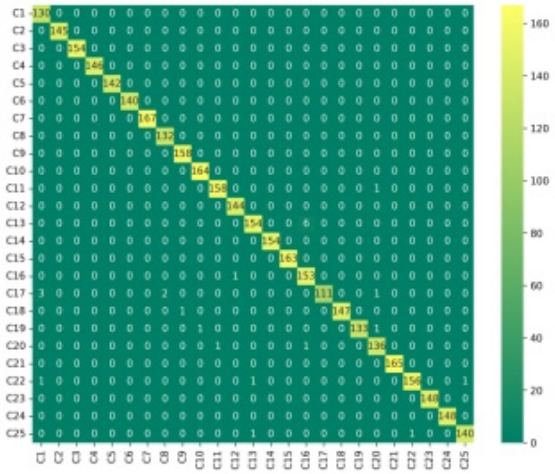

**Fig 6.** 30dB

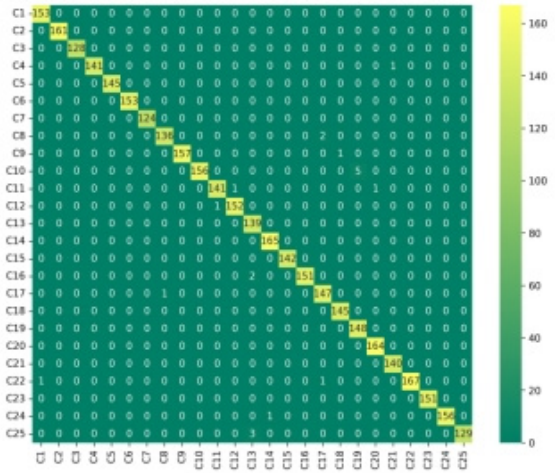

**Fig 7.** 50dB

**Table 3.** Accuracy of each comparative model under three signal-to-noise ratio conditions

| Model name | Classification accuracy/% | | |
|---|---|---|---|
| | 20 dB | 30 dB | 50 dB |
| CNN | 87.74 | 89.88 | 92.46 |
| LSTM | 86.23 | 91.82 | 93.36 |
| TCN+LSTM | 93.67 | 96.12 | 98.34 |
| CNN-Transformer | 91.82 | 93.76 | 95.58 |
| MCA-KAN | 97.82 | 99.39 | 99.56 |

In a 20dB noise environment, the model achieves a recognition accuracy of 97.82%, outperforming CNN, LSTM, TCN+LSTM, and CNN-Transformer by 10.84%, 11.99%, 4.55%, and 6.4% respectively under identical conditions.

The table demonstrates the exceptional robustness of the MCA-KAN model. When noise levels are high (e.g., 20 dB SNR), while other models show a significant drop in classification accuracy, MCA-KAN maintains high accuracy. Moreover, under 30 dB and 50 dB noise conditions, the proposed model continues to outperform other classification models. By incorporating cross-attention mechanisms and KANLinear layers, MCA-KAN enables adaptive integration of time-domain and frequency-domain features, effectively enhancing its noise resistance.

# 4. Conclusion

This study proposes a Multi-Channel Attention Mechanism and KAN Network-based Power Quality Disturbance Classification Model (MCA-KAN) to improve the accuracy and robustness of power quality disturbance classification in high-noise environments. By integrating time-domain convolutional neural networks, frequency-domain convolutional neural networks, bidirectional Long Short-Term Memory (LSTM) networks, and cross-attention mechanisms, MCA-KAN efficiently extracts critical information from time-frequency domain features. The nonlinear mapping through the KAN Linear layer significantly enhances the model's classification performance.

Experimental results demonstrate that MCA-KAN achieves outstanding performance across various signal-to-noise ratio (SNR) conditions. Notably, it achieves 97.82% accuracy at 20dB noise level, significantly outperforming traditional models including CNN, LSTM, and TCN+LSTM. Confusion matrix analysis further reveals that the model exhibits near-perfect classification performance under high SNR conditions while maintaining robustness even at low SNR levels.

While the MCA-KAN model has demonstrated strong performance in current experiments, there remains room for improvement. Future research could explore incorporating additional data augmentation techniques to enhance its adaptability to complex perturbation signals. Furthermore, integrating other deep learning models (such as graph neural networks) may further improve the model's performance, particularly when processing real-time data in large-scale power systems.

# References


[1] Han Yu, Zhou Qian, Li Yong, et al. Analysis of power quality issues and quantified evaluation of additional losses in low-voltage distribution networks for household photovoltaic integration [J]. Journal of Electric Power Science and Technology, 2024,39(03):177-186.

[2] Mahela O P, Shaik A G, Gupta N. A critical review of detection and classification of power quality events[J]. Renewable and Sustainable Energy Reviews, 2015, 41: 495-505.

[3] Zhang Y, Zhang Y, Zhou X. Classification of power quality disturbances using visual attention mechanism and feed-forward neural network[J]. Measurement, 2022, 188: 110390.

[4] Wang Y. A Review of Research on Power Quality Disturbance Detection [J]. Power System Protection and Control, 2021,49(13):174-186.

[5] Wang M, Zhou H, Yang S, et al. Robust compressive features based power quality events classification with Analog–Digital Mixing Network (ADMN)[J]. Neurocomputing, 2016, 171: 685-692.

[6] Sun Dong, Gao Qingwei, Zhu De, et al. Adaptive cyclic power harmonic analysis algorithm based on discrete Fourier transform [J]. Journal of Anhui University (Natural Science Edition), 2013,37(06):57-64.

[7] De Yong D, Bhowmik S, Magnago F. An effective power quality classifier using wavelet transform and support vector machines[J]. Expert Systems with Applications, 2015, 42(15-16): 6075-6081.

[8] Xu Liwu, Li Kaicheng, Luo Yi, et al. Composite power quality disturbance recognition based on incomplete S-transform and gradient boosting tree [J]. Power System Protection and Control, 2019,47(06):24-31.

[9] Samanta I S, Rout P K, Swain K, Samanta I S, Rout P K, Swain K, et al. Power quality events recognition using enhanced empirical mode decomposition and optimized extreme learning machine[J]. Computers and Electrical Engineering, 2022, 100: 107926.

[10] Carní D L, Lamonaca F. Toward an automatic power quality measurement system: An effective classifier of power signal alterations[J]. IEEE Transactions on Instrumentation and Measurement, 2022, 71: 1-8.

[11] Sahani M, Dash P K. Automatic power quality events recognition using modes decomposition based online P-norm adaptive extreme learning machine[J]. IEEE Transactions on Industrial Informatics, 2019, 16(7): 4355-4364.

[12] Gonzalez-Abreu A D, Saucedo-Dorantes J J, Osornio-Rios R A, et al. Condition monitoring approach based on dimensionality reduction techniques for detecting power quality disturbances in cogeneration systems[C]//2019 24th IEEE International Conference on Emerging Technologies and Factory Automation (ETFA). IEEE, 2019: 898-903.

[13] Minh Khoa N, Van Dai L. Detection and classification of power quality disturbances in power system using modified-combination between the stockwell transform and decision tree methods[J]. Energies, 2020, 13(14): 3623.

[14] Choudhary B. Choudhary B. An advanced genetic algorithm with improved support vector machine for multi-class classification of real power quality events[J]. Electric Power Systems Research, 2021, 191: 106879.

[15] Lin L, Wang D, Zhao S, Lin L, Wang D, Zhao S, et al. Power quality disturbance feature selection and pattern recognition based on image enhancement techniques[J]. Ieee Access, 2019, 7: 67889-67904.

[16] Cai K, Cao W, Aarniovuori L, Cai K, Cao W, Aarniovuori L, et al. Classification of power quality disturbances using Wigner-Ville distribution and deep convolutional neural networks[J]. IEEe Access, 2019, 7: 119099-119109.

[17] Shukla J, Panigrahi B K, Ray P K. Power quality disturbances classification based on Gramian angular summation field method and convolutional neural networks[J]. International Transactions on Electrical Energy Systems, 2021, 31(12): e13222.

[18] Yuan D, Liu Y, Lan M, Yuan D, Liu Y, Lan M, et al. A novel recognition method for complex power quality disturbances based on visualization trajectory circle and machine vision[J]. IEEE transactions on instrumentation and measurement, 2022, 71: 1-13.

[19] Zhou L, Gu S, Liu Y, et al. A novel recognition method for complex power quality disturbances based on Markov transition field and improved densely connected network[J]. Frontiers in Energy Research, 2024, 12: 1328994.

[20] Mohan N, Soman K P, Vinayakumar R. Deep power: Deep learning architectures for power quality disturbances classification[C]//2017 international conference on technological advancements in power and energy (TAP Energy). IEEE, 2017: 1-6.

[21] Chiam D H, Lim K H, Law K H. LSTM power quality disturbance classification with wavelets and attention mechanism[J]. Electrical Engineering, 2023, 105(1): 259-266.

[22] Cabral T W, Gomes F V, de Lima E R, Cabral T W, Gomes F V, de Lima E R, et al. Kolmogorov–Arnold Network in the Fault Diagnosis of Oil-Immersed Power Transformers[J]. Sensors, 2024, 24(23): 7585.